© 2016. Published by The Company of Biologists Ltd | Journal of Cell Science (2016) 129, 681-692 doi:10.1242/jcs.175745

RESEARCH ARTICLE

Evidence for a dual role of actin in regulating chromosome organization and dynamics in yeast

Maya Spichal[1,2,3,4,5,6], Alice Brion[1,2,3], Sébastien Herbert[7,8], Axel Cournac[4,5], Martial Marbouty[4,5], Christophe Zimmer[7,8], Romain Koszul[4,5,*] and Emmanuelle Fabre[1,2,3,4,5,*]

ABSTRACT

Eukaryotic chromosomes undergo movements that are involved in the regulation of functional processes such as DNA repair. To better understand the origin of these movements, we used fluorescence microscopy, image analysis and chromosome conformation capture to quantify the actin contribution to chromosome movements and interactions in budding yeast. We show that both the cytoskeletal and nuclear actin drive local chromosome movements, independently of Csm4, a putative LINC protein. Inhibition of actin polymerization reduces subtelomere dynamics, resulting in more confined territories and enrichment in subtelomeric contacts. Artificial tethering of actin to nuclear pores increased both nuclear pore complex (NPC) and subtelomere motion. Chromosome loci that were positioned away from telomeres exhibited reduced motion in the presence of an actin polymerization inhibitor but were unaffected by the lack of Csm4. We further show that actin was required for locus mobility that was induced by targeting the chromatin-remodeling protein Ino80. Correlated with this, DNA repair by homologous recombination was less efficient. Overall, interphase chromosome dynamics are modulated by the additive effects of cytoskeletal actin through forces mediated by the nuclear envelope and nuclear actin, probably through the function of actin in chromatin-remodeling complexes.

KEY WORDS: Actin, Chromosome, Dynamics

INTRODUCTION

All genomes exhibit multiple levels of organization. Dynamic changes of this organization are observed concomitantly with the proceeding of most, if not all, DNA-related metabolic processes, such as replication, transcription and repair. Experimental evidence points to a role of this dynamic organization in the functional regulation of these important processes (Soutoglou and Misteli, 2007). Hence, the origin of chromosome dynamics is being increasingly investigated, with important efforts aiming to characterize both active and passive mechanisms (for reviews, see Chuang and Belmont, 2007; Zimmer and Fabre, 2011). Chromatin exhibits stochastic movements that are qualitatively consistent with confined diffusion or subdiffusion and thermal agitation (Cabal et al., 2006; Marshall et al., 1997). However, evidence for active, ATP-dependent movements have also been reported in both mitotic (Heun et al., 2001; Weber et al., 2012; Zidovska et al., 2013) and meiotic cells in yeast, worms and mammals (Conrad et al., 2008; Koszul et al., 2008).

In this study, we aimed at further investigating the potential influence of actin on chromosome dynamics. In the cytoplasm, actin exists in a dynamic interplay between its monomeric form, G-actin, and its polymerized form F-actin. F-actin is a complex cytoskeletal structure involved in a variety of conserved functions, including endocytosis, cytoplasmic transport and nuclear migration (for reviews, see Mishra et al., 2014; Stricker et al., 2010). The presence of actin in the nucleus, once a hotly debated topic, is now established, primarily from studies in mammalian cells (for review, see de Lanerolle, 2012). In contrast to cytoplasmic actin, most nuclear actin exists in its monomeric form. Yet, actin filaments have been found in the nucleus of certain cell types (for review, see Grosse and Vartiainen, 2013). For instance, formin–actin rods can be detected under non-physiological conditions, such as heat shock, ATP depletion or inhibition of actin polymerization with latrunculin A (de Lanerolle, 2012; Grosse and Vartiainen, 2013). Nuclear actin filaments are also formed upon serum stimulation of quiescent fibroblasts, a step that is involved in the regulation of actin-binding transcription factor MRTF (Baarlink et al., 2013). Furthermore, G-actin and actin related proteins (Arps) are part of chromatin-remodeling complexes, which are conserved from yeast to mammals (for review, see Kapoor and Shen, 2014). Nuclear actin has also been shown to modulate transcription through binding to all three classes of RNA polymerase and through regulation of chromosome movement (Chuang et al., 2006; Dundr et al., 2007). Actin nuclear import and export, mediated by the actin-binding proteins cofilin and profilin, appears to play a role in the regulation of nuclear actin (Baarlink et al., 2013; de Lanerolle and Serebryannyy, 2011).

Unlike mammalian species, the yeast genome carries a single essential gene, *ACT1*, encoding actin. The yeast Act1 protein is found in NuA4, a histone acetyl transferase complex, as well as in the chromatin-remodeling complexes SWR1 and INO80. The INO80 complex is involved in DNA repair, replication and cell-cycle control (for review, see Dion and Gasser, 2013). *In vitro*, interaction of the Ino80 subunit with chromatin has been shown to require the actin module containing Arp4 and Arp8 (Kapoor et al., 2013). Targeting of Ino80 to a given locus *in vivo* enhances motion of the locus, through a process involving the ATPase activity of Ino80 (Neumann et al., 2012). The exact role of actin in regulating these functions is, however, unclear, notably its influence on chromosome dynamics.

One of the mechanisms that links the cytoskeleton to chromosomes functions through proteins that contain SUN and KASH domains. These proteins, located in the nuclear envelope, form a linker of nucleoskeleton and cytoskeleton (LINC) complex that physically connects the cytoskeleton to chromosomes. During

[1]INSERM UMR 944, Equipe Biologie et Dynamique des Chromosomes, Institut Universitaire d'Hématologie, Hôpital St. Louis 1, Avenue Claude Vellefaux, Paris 75010, France. [2]CNRS, UMR 7212, Paris 75010, France. [3]Université Paris Diderot, Sorbonne Paris Cité, Paris 75010, France. [4]Institut Pasteur, Groupe Régulation Spatiale des Génomes, Paris 75015, France. [5]CNRS, UMR 3525, Paris 75015, France. [6]Sorbonne Universités, UPMC Université Paris 6, Paris 75005, France. [7]Institut Pasteur, Unité Imagerie et Modélisation, Paris 75015, France. [8]CNRS, URA 2582, Paris 75015, France.

*Authors for correspondence (romain.koszul@pasteur.fr; emmanuelle-g.fabre@inserm.fr)

Received 12 June 2015; Accepted 5 January 2016

Journal of Cell Science (2016) 129, 681-692 doi:10.1242/jcs.175745

meiotic prophase, a dynamic reorganization of the chromosomes is ensured by the LINC complex (Horn et al., 2013; Rog and Dernburg, 2013; Sheehan and Pawlowski, 2009). In budding yeast, *Saccharomyces cerevisiae*, these movements are driven by forces generated at the level of the actin cytoskeleton and transduced through the nuclear envelope and Csm4 to the telomeres (Conrad et al., 2008; Koszul et al., 2008; Scherthan, 2007; Trelles-Sticken et al., 2000).

During interphase of yeast vegetative cells, dynamic interactions of chromosomes with the nuclear envelope are observed, but the rapid global movements described in meiosis remain specific to that cell stage. The dynamics of discrete chromosomal loci depend on their chromosomal and nuclear position, for which the nuclear envelope appears to play a crucial role. More specifically, the 32 chromosome ends of a haploid *S. cerevisiae* genome are tethered to the nuclear envelope through redundant pathways that involve Esc1, Mps3, Csm4, the silencing informatory regulator (Sir) proteins and the nuclear pore complex (NPC) (Bupp et al., 2007; Feuerbach et al., 2002; Galy et al., 2000; Hediger et al., 2002; Hiraga et al., 2008; Taddei et al., 2004; Therizols et al., 2006; Van de Vosse et al., 2013). As a result of their attachment to the nuclear envelope, subtelomere movements occur within a relatively confined environment (Heun et al., 2001; Therizols et al., 2010).

Here, we investigate the role of actin and Csm4 in the dynamics and organization of chromosomes in the *S. cerevisiae* nucleus through a combination of cellular imaging and genetic techniques. We show that the diffusion of NPCs is reduced in the absence of polymerized actin, whereas the bridging of actin filaments to NPCs increases their diffusion. Such a bridge increases subtelomere dynamics but not that of an internal locus. Interestingly, the presence of latrunculin A reduces the movement of chromosomal regions located far from the nuclear envelope. Inhibition of actin polymerization also remodels the nuclear territories of subtelomeres in both wild type (WT) and Δ*csm4* cells, pointing to a role of actin in actively increasing the territories explored by chromosome loci during interphase. In these conditions, contacts between subtelomeres increase. The presence of latrunculin A prevents local mobility owing to targeted complex-remodeling protein Ino80. In these conditions, targeted homologous recombination following induced double-strand breaks (DSBs) is reduced. We show that actin is required for active chromosome dynamics and suggest that motion is generated by an additive effect at the cytoplasmic level, possibly transduced to subtelomeres through the nuclear envelope and NPCs and, in the nucleus, probably through chromatin-remodeling complex functions.

RESULTS

Antagonistic effects of Csm4 and polymerized actin on subtelomere dynamics

To investigate the potential role(s) of actin in controlling chromosome motion, we monitored the dynamics of three subtelomeric loci labeled with the fluorescent repressor–operator system (FROS) comprising a GFP-tagged tetracycline repressor and tetracycline operator (TetO/TetR–GFP) (Michaelis et al., 1997). Chromosome extremities are known to be positioned close to the nuclear periphery and in the vicinity of NPCs (Bupp et al., 2007; Feuerbach et al., 2002; Galy et al., 2000; Hediger et al., 2002; Hiraga et al., 2008; Taddei et al., 2004; Therizols et al., 2010; Van de Vosse et al., 2013), and could therefore be more sensitive to actin cytoskeleton defects. The loci were chosen on chromosome arms of different lengths, ranging from short to long (Tel14R, 157 kb; Tel5R, 430 kb; Tel15R, 705 kb; Fig. 1A; Fig. S1A). To deplete actin filaments, we incubated the cells at room temperature in the presence of 30 µM latrunculin A (hereafter referred to as Lat) for 30 min before imaging and monitored drug efficiency with actin-binding protein Abp140p. Lat was preferred over other actin depolymerizing drugs (cytochalasin, swinholide) because of its ability to bind to and trap actin monomers specifically through its insertion into the barbed end of actin (Morton et al., 2000). As a control, cells were incubated in Lat solvent, DMSO (Fig. 1A). The movements of subtelomeres were tracked using time-lapse fluorescence microscopy in 500–1500 cells, and the mean square displacements (MSD) were computed (Fig. 1B; Fig. S1A; Materials and Methods). In both WT and Lat-treated cells, the MSD revealed a consistent scaling law with time interval Δt, $MSD \approx 4C\Delta t^{\alpha}$ described by an exponent $\alpha \approx 0.5$ (Materials and Methods). The prefactor C characterizes how fast the chromatin locus moves, the exponent is indicative of the type of diffusion, subdiffusive if $\alpha<1$ or diffusive if $\alpha=1$ (in this latter case, C would be identical to the diffusion coefficient). Our finding that $\alpha \approx 0.5$ is in agreement with previous studies on other chromosome loci, which have reported subdiffusion with similar exponents in both prokaryotes and eukaryotes (Cabal et al., 2006; Hajjoul et al., 2013; Weber et al., 2010). This shows that subtelomeres undergo subdiffusive motion. Interestingly, subtelomere dynamics in Lat-treated cells remained subdiffusive with the same exponent $\alpha \approx 0.5$; the prefactor C substantially decreased in the presence of latrunculin, indicating a reduced motion of the chromatin locus (Fig. 1B, Table 1; Fig. S1A).

During yeast meiotic prophase, the actin cytoskeleton drives movements of the nuclear envelope LINC complex (Conrad et al., 2008; Koszul et al., 2008). To test whether a similar interplay determines subtelomeric dynamics during vegetative growth, the imaging analysis was performed in Mps3 and Csm4 mutant strains, two members of the LINC complex whose absence impairs meiotic movements (Conrad et al., 2008; Wanat et al., 2008). $\Delta N_{1\text{-}75}$*mps3* mutants quickly accumulate aneuploid chromosomes. This phenotype can be rescued in a mutant of the NPC, Δ*pom152* (Fig. S2; Witkin et al., 2010). Yet, Δ*pom152* itself has an effect on subtelomere organization (Fig. S2), making it difficult to non-ambiguously interpret the role of $\Delta N_{1\text{-}75}$*mps3* in subtelomere positioning in the double mutant. Therefore, this mutant was discarded from further analysis. In contrast, Δ*csm4* did not accumulate chromosomal defects. Subtelomeric subdiffusion appeared to be faster in Δ*csm4* than in WT (Fig. 1B). Further analyses of subtelomere organization in this mutant revealed a release from the nuclear envelope (see below, Fig. 1C, Table 1; Fig. S1), confirming and extending previous observations of a delocalization of the long chromosome arm subtelomere Tel14L in the absence of Csm4 (Hiraga et al., 2008). Our results show that Csm4 is important for subtelomere positioning and for constrained dynamics. Interestingly, in the presence of latrunculin, subtelomere dynamics were decreased in Δ*csm4* (Fig. 1B). This indicates a synergistic rather than an epistatic influence between defects in actin polymerization and the Δ*csm4* mutant.

Altogether, these results point to an influence of actin filaments on subtelomere dynamics during interphase that is distinct from that one observed during meiotic prophase.

Csm4 and actin differentially modulate the characteristics of subtelomeric territories

To determine the impact of the decreased chromosome mobility on their overall organization, the territories occupied in the nuclear space by the subtelomeres were computed from thousands of cells using nucloc, an automated image analysis program (Berger et al., 2008;

Journal of Cell Science (2016) 129, 681-692 doi:10.1242/jcs.175745

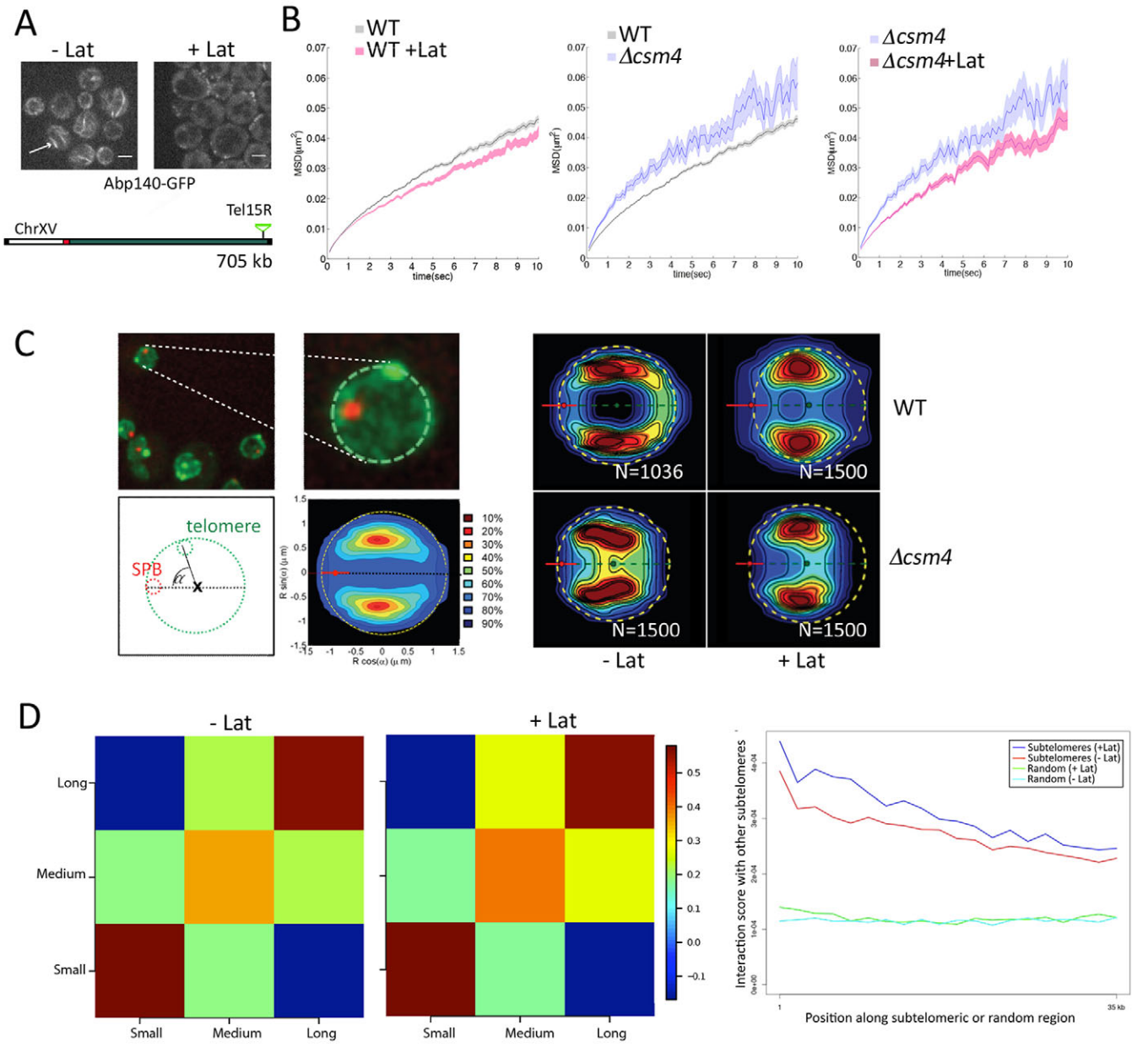

Fig. 1. Subtelomere motion and territory are differentially affected in the absence of polymerized actin or KASH-like protein Csm4, and subtelomere–subtelomere contacts are increased in the absence of polymerized actin. (A) Top, actin filaments visualized by staining for Abp140 (arrow) are lost upon latrunculin A treatment (+Lat). Scale bar: 1 µm. Bottom, schematic of the TetO/TetR–GFP-labeled subtelomere Tel15R located on the long right arm of chromosome XV in *S. cerevisiae*. Size is indicated in kb on the right, the centromere as a red dot, the TetO/TetR–GFP arrays as a green triangle and telomeres as black boxes. (B) MSD after tracking spots in 2D time-lapse video (10 Hz) in 500–1000 cells in untreated WT cells (grey, WT) or in the presence of latrunculin A (pink, WT +Lat), in the Δ*csm4* mutant strain without latrunculin A (blue, Δ*csm4*) and in the presence of latrunculin A (pink, Δ*csm4* +Lat). Nuclei displacements were corrected, and one-third of the curve was taken into consideration to fit α and C (subdiffusion coefficient). Shaded area around the lines represent ±s.e.m. (C) Nuclear territories mapped by automated analysis of 3D images of ∼750–1500 nuclei using the nucloc software (Berger et al., 2008; Therizols et al., 2010). Left, in each nucleus, the SPB is visible as a red dot on the 3D projection of a *z*-stack. Nucloc uses 3D coordinates of the SPB together with the center of mass of the nucleus to orient each nucleus and to generate probability maps of loci positions. Right, locus probability maps of synchronized G1 cells under different conditions, WT and Δ*csm4* with (+Lat) or without (–Lat) latrunculin B. The dark red area in each map has the highest probability density and contains the locus in 10% of nuclei. *N* is the total number of analyzed nuclei. (D) Left, correlation matrices of subtelomere–subtelomere contacts with and without latrunculin A from genome-wide chromosome conformation capture (3C-seq analysis). Subtelomeres are sorted according to their chromosome arm length into three subgroups. The first group corresponds to the smallest arms ranging from 80 kb (Tel1R) to 155 kb (Tel14R). The second group corresponds to arms of intermediate size ranging from 202 kb (Tel3R) to 355 kb (Tel9L). The last group corresponds to telomeres of the longest arms ranging from 392 kb (Tel16R) to 1082 kb (Tel4R). Right, interaction score according to genomic position on subtelomeres. Correlation matrices with ungrouped subtelomeres are shown in Fig. S1D.

Fig. 1C; Fig. S1B). Briefly, for each nucleus, the relative position of a fluorescently labeled locus with respect to two nuclear landmarks was determined from three-dimensional (3D) microscopy images. Analyzed in over hundreds of cells, these positions were then aggregated to generate two-dimensional (2D) probability density maps. Here, the spindle pole body (SPB; the yeast microtubule organizing center) was used as one of the two nuclear landmarks (the second one being the center of the nucleus), instead of the nucleolus

Journal of Cell Science (2016) 129, 681-692 doi:10.1242/jcs.175745

Table 1. Subdiffusive motion of loci examined in this study

Locus	Distance from centromere (kb)	Prefactor C ($\mu m^2/sec^{0.5}$)	s.e.m.	Number of cells
Tel15R (DMSO)	705	2.94×10^{-3}	4.45×10^{-5}	2012
Tel15R (+Lat)	705	2.63×10^{-3}	5.44×10^{-5}	1164
Tel15R Δ*csm4* (DMSO)	705	3.82×10^{-3}	2.04×10^{-4}	86
Tel15R Δ*csm4* (+Lat)	705	2.86×10^{-3}	1.11×10^{-4}	304
Mid (YDR336w) (DMSO)	695	4.69×10^{-3}	8.68×10^{-5}	788
Mid (YDR336w) (+Lat)	695	4.01×10^{-3}	9.20×10^{-5}	524
Mid (YDR336w) Δ*csm4* (DMSO)	695	6.28×10^{-3}	1.09×10^{-4}	446
Mid (YDR336w) Δ*csm4* (+Lat)	695	4.99×10^{-3}	1.04×10^{-4}	322
Mid (YDR336w) Δ*csm4*	695	7.44×10^{-3}	1.20×10^{-4}	479
Mid (YDR336w)	695	7.41×10^{-3}	1.35×10^{-4}	396
Mid (YDR336w) LGN	695	7.15×10^{-3}	1.36×10^{-4}	346
Cen+LexA	12	4.76×10^{-3}	2.84×10^{-4}	63
Cen+LexA–Ino80	12	6.28×10^{-3}	3.94×10^{-4}	44
Cen+LexA–Ino80+Lat	12	4.37×10^{-3}	1.19×10^{-4}	361
Cen+LexA+Lat	12	4.27×10^{-3}	1.21×10^{-4}	302
Tel14R (DMSO)	157	3.11×10^{-3}	7.70×10^{-5}	876
Tel14R (+Lat)	157	2.68×10^{-3}	7.11×10^{-5}	862
Tel14R Δ*csm4* (DMSO)	157	3.79×10^{-3}	9.23×10^{-5}	606
Tel5R (DMSO)	430	2.38×10^{-3}	3.35×10^{-5}	3068
Tel5R (+Lat)	430	2.21×10^{-3}	3.41×10^{-5}	3246
Tel5R Δ*csm4* (DMSO)	430	3.01×10^{-3}	1.04×10^{-4}	323
Tel15R LGN (DMSO)	705	3.42×10^{-3}	1.79×10^{-4}	147
Tel15R LGN (+Lat)	705	2.61×10^{-3}	1.16×10^{-4}	241

Genomic position is indicated as a distance from the centromere. s.e.m., standard error of the mean of the prefactor C value. Cen, centromere; Lat, latrunculin A; LGN, LifeAct–GFP–Nup49 construct.

as center of mass as initially used by Berger et al. (2008). The Spc29–mCherry fluorescently labeled SPB appeared as a diffraction-limited discrete fluorescent complex facing the nucleolus (Fig. 1C). Data acquisition was performed on G1-phase daughter cells that had been recovered through centrifugal elutriation to avoid potential nuclear deformations resulting from hormonal treatment (Marbouty et al., 2014). As expected, these cells exhibited a single discrete fluorescent SPB that was used as a landmark to generate high-resolution probabilistic 2D maps (Fig. 1C; Fig. S1B,C). Furthermore, the three subtelomeres were positioned on average in the vicinity of the nuclear envelope, with the chromosome arm lengths influencing the average angular positions with respect to the SPB–nuclear-center axis (Fig. 1C; Fig. S1B; Therizols et al., 2010).

To reduce subtelomere mobility, cells were then incubated at room temperature in the presence or absence of latrunculin B (see Materials and Methods). In the presence of latrunculin B, the subtelomere territories remained at the nuclear periphery and were correlated to chromosome arm length (Fig. 1C; Fig. S1B). Yet, statistical tests revealed that territories occupied by long and middle arm subtelomeres (i.e. Tel15R and Tel5R) were significantly modified [*P*-values of 9.7×10^{-7} (long arm) and 1.8×10^{-4} (middle arm) between WT and latrunculin-B-treated conditions; see Materials and Methods, and Duong et al., 2012]. Interestingly, the volumes occupied by the territories were also significantly reduced in the presence of latrunculin B (2.3–1.5 μm^3 and 2.5–2.1 μm^3 for Tel15R and Tel5R, respectively; Table S1; Berger et al., 2008). For the short arm Tel14R territory, no significant effects were observed (Fig. S1A; $P=0.425$), perhaps reflecting the stronger mechanical constraints exerted on small chromosome arms as a result of the higher density of chromatin in the vicinity of the SPB, where all chromosome arms are tethered (Wong et al., 2012).

To test the effect of actin depolymerization on untethered subtelomeres, we characterized subtelomere territories in the absence of Csm4 in the G1 phase. In a Δ*csm4* background, territories occupied by the middle and long chromosome arm subtelomeres drifted away from the nuclear membrane, as shown by computing the median distance between the center of the territory and the nuclear envelope (shift from 0.192 µm to 0.186 µm, 0.179 to 0.205 and 0.197 to 0.245 for Tel14R, Tel5R and Tel15R, respectively; Fig. 1C; Fig. S1B; Table S1). Interestingly, treatment with latrunculin B in the absence of Csm4 further reduced the volume and increased the confinement of Tel5R and Tel15R territories (by −8% and −14%, respectively; Table S1). Therefore, actin depolymerization affects subtelomere organization independently of nuclear envelope targeting during G1-phase vegetative growth.

Actin-mediated subtelomere dynamics determine subtelomere–subtelomere interactions

Collisions between subtelomeres involve more frequently chromosome arms of similar sizes (Hoze et al., 2013; Therizols et al., 2010). Using genome-wide chromosome conformation capture (3C) experiments, we quantified the average contact frequencies between subtelomeres in populations of cells under WT and latrunculin-A conditions (Material and Methods; Duan et al., 2010; Marie-Nelly et al., 2014). Contacts between subtelomeric regions (i.e. 30-kb windows starting from the telomere) were computed and maps generated with the subtelomeres sorted according to their chromosome arm length (Fig. 1D; Fig. S1D). In untreated cells, two groups of subtelomeres displayed enriched contact frequencies among themselves, corresponding to short (<150 kb) and long (>300 kb) arms (brown squares, Fig. 1D, left; Duan et al., 2010; Therizols et al., 2010), whereas lat-treated cells reproducibly exhibited a substantial increase in subtelomere–subtelomere contacts (by about 10–30%, Fig. 1D, right). Therefore, the reduced dynamics associated with the presence of latrunculin A correlates with an increase in contacts between the subtelomeres of chromosome arms with similar sizes.

Nuclear pore dynamics decrease in the absence of actin filaments

For the actin cytoskeleton network to influence subtelomere motion, mechanical forces have to propagate through the nuclear envelope.

Journal of Cell Science (2016) 129, 681-692 doi:10.1242/jcs.175745

Because Csm4, which plays such a role during meiosis prophase, did not appear to do so in G1, we examined NPC dynamics under conditions that affect actin filament formation. We characterized the mobility of wild-type NPCs in both tropomyosin mutants and under latrunculin-A-treated conditions. Tropomyosin stabilizes actin cables and is encoded by the paralogous genes *TPM1* and *TPM2* (Drees et al., 1995). At 34.5°C, actin filaments are destabilized in the thermosensitive strain Δ*tpm2 tpm1-1* (Pruyne et al., 1998). Actin cables were labeled using Abp140–GFP (Riedl et al., 2008). Cytoplasmic actin cables were depleted both in tropomyosin mutants at the non-permissive temperature and in the presence of latrunculin A (Fig. 2). NPC diffusion was visualized with nucleoporin Nup49 fused to GFP (Nup49–GFP) and by fluorescence recovery after photobleaching (FRAP) of a region of the nuclear envelope (Materials and Methods) in WT cells and under actin-depolymerizing conditions (Fig. 2A). To compare quantitatively different situations, we considered the fluorescence recovered after 30 s. In WT or tropomyosin mutant cells, grown at 30°C, 30%±3% fluorescence was recovered after 30 s. Nuclear pore mobility was compromised upon addition of latrunculin A to a WT culture (20%±3%, Fig. 2B) or in tropomyosin mutant cells at the restrictive temperature (20%±1.5%, Fig. 2D). Deletion of nuclear envelope components, Δ*csm4* (Fig. 2B) or members of the NPC (Δ*pom152*; Δ*nup170*) did not result in significant effects on nuclear pore diffusion (Fig. S3, see Discussion). Furthermore, nuclear pore dynamics remained unchanged in a background in which the chromatin-remodeling complex INO80 was compromised (Δ*arp8*, Fig. S3). These results show that actin cytoplasmic filaments are required for nuclear pore diffusion.

Artificial tethering of actin to the nuclear envelope increases NPC diffusion and subtelomere dynamics

Having shown that lack of actin filaments impairs NPC and subtelomere dynamics, we sought to obtain direct evidence of the mechanical link between nuclear pore diffusion and subtelomere dynamics. In order to see if increasing the nuclear pore dynamics would result in an increase in chromosome mobility, we anchored actin to Nup49. To do so, the actin-cable-binding domain LifeAct (Riedl et al., 2008) was fused to Nup49–GFP and put under the control of the wild-type *NUP49* promoter (LifeAct–GFP–Nup49, hereafter named LGN) in a Δ*nup49* background (Fig. 3). Given the fact that *NUP49* is essential for cell survival, we first constructed two shuffling strains in which Δ*nup49* was complemented by two plasmids, one expressing wild-type Nup49 and another expressing either Nup49–GFP or LGN. If LGN can efficiently complement Δ*nup49*, it should be possible to recover cells that express only LGN. This was the case with a frequency of spontaneous loss three times more efficient for Nup49–GFP (40% and 13.5% for Nup49-GFP and LGN, respectively). The respective division times were 1h 45 min and 2 h 20 min for cells expressing Nup49–GFP and cells expressing the LGN fusion protein. As observed with fluorescence and confirmed with structured illuminated microscopy (SIM), LGN concentrated into bright discrete structures at the NPC that colocalized with another integral component of NPC fused to a red variant, Nup159–mCherry (Fig. 3; Hayakawa et al., 2012). Interestingly, the nuclear envelope exhibited important deformations, with elongated structures reminiscent of those observed in an *Δndj1* mutant during meiotic prophase, where subtelomeres are detached from the LINC complex, but actin cables keep pulling on the nuclear envelope external membrane, leading to nuclear envelope deformations (Koszul et al., 2008). In LGN-expressing cells, the nuclear envelope deformations were lost upon treatment with latrunculin A (Fig. S4). We conclude that LGN is a functional NPC protein and that its ability to connect to actin filaments modifies the morphology of the nuclear envelope. Nup49–GFP and LGN diffusion dynamics were then followed by using FRAP. FRAP experiments first revealed an increase in NPC diffusion in the strain expressing LGN compared to the strain that did not (+ and −LGN, respectively; Fig. 3B). NPC diffusion was greatly diminished in the presence of latrunculin A (Fig. S4). These observations indicate that LGN favors actin filament attachment to the nucleus and consequently Nup49–GFP diffusion in the nuclear membrane.

We then tested whether the LGN construct had an effect on subtelomere dynamics. The MSD of subtelomere Tel15R was characterized in the presence or absence of LGN. Subtelomere dynamics remained subdiffusive with a power of law of $\alpha \approx 0.5$, the subdiffusion coefficient increased significantly (*P*-value Kolmogorov–Smirnov test=0.0065; Fig. 3). In addition, subtelomere dynamics decreased in the presence of latrunculin A (Fig. S4). Altogether, these results establish that NPC association to the cytoskeleton influences both NPC and subtelomere motion, pointing at the nuclear envelope as a regulator of subtelomere dynamics.

Internal chromosome loci dynamics are reduced in the absence of polymerized actin but not in the absence of Csm4

The links between actin cytoskeleton, NPC and subtelomere dynamics prompted us to analyze the motion of other chromosomal loci distant from the telomere, in the presence and absence of filamentous actin. A position within the right arm of chromosome IV, known to be preferentially positioned away from the periphery (735 kb from the centromere; Wong et al., 2012) was tracked by using time-lapse acquisition as described above, with or without latrunculin A (Materials and Methods). In the DMSO control, all loci exhibited similar prefactor C values in agreement with previous results (above and Hajjoul et al., 2013). Interestingly, in the presence of latrunculin A, a marked decrease in subdiffusion was observed both in WT and Δ*csm4* cells (Fig. 4A; Fig. S1, Table S1). However, in the absence of treatment with latrunculin A, the movement of the middle chromosomal arm site was unaltered in Δ*csm4* (Fig. 4B), indicating that this putative KASH ortholog is not involved in chromosome dynamics in general.

The effect of latrunculin A on the dynamics of chromosomal loci in interstitial regions points to two possible scenarios. Either the influence of actin inside the nuclear space results from the forces generated at the level of cytoplasmic actin filaments that are transduced to chromosomes, extending from subtelomeres to the entire chromosome, or alternatively this effect could result from the sequestration of nuclear monomeric actin by latrunculin. Indeed, the size of the latrunculin A molecule does allow its diffusion into the nucleus (Morton et al., 2000). The former scenario appears unlikely given that the dynamics of an internal locus is unaffected by the expression of LGN (Fig. 4B). Therefore, a likely effect of latrunculin A is that it impacts on the chromosome dynamics of all interstitial loci studied through the sequestration of nuclear actin.

Actin is required for chromosomal movements induced by fusion of the chromatin remodeling protein Ino80 to LexA

To address whether nuclear actin plays a role in chromosome mobility through chromatin-remodeling complexes, we implemented the LexA–Ino80 system described previously by Neumann et al. (2012; Methods). This system allows us to affect the mobility of a locus by targeting it with the Ino80 protein, the ATPase of the

Journal of Cell Science (2016) 129, 681-692 doi:10.1242/jcs.175745

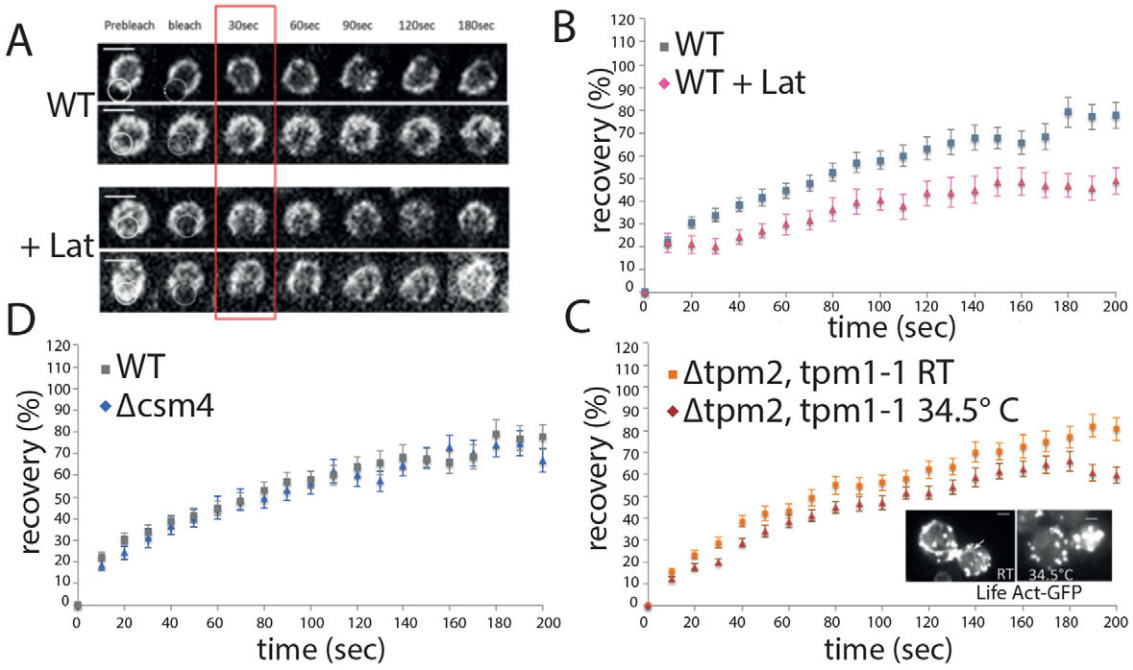

Fig. 2. Nuclear pore mobility is compromised in the absence of actin filaments but not in the absence of Csm4. (A) Images from movies of FRAP for NUP49–GFP-labeled cells (WT) that had been treated with DMSO or 30 µM latrunculin A for 30 min (+Lat). (B) FRAP analyses of Nup49–GFP (WT) cells treated with DMSO and latrunculin A (+Lat). The curves are the mean± s.e.m.; WT+DMSO, *n*=37; WT+latrunculin A, *n*=15. (C) Depolymerization of actin cables in tropomyosin thermosensitive mutants (at 34.5°) was followed with LifeAct–GFP. Actin filaments were visible at room temperature (arrow) and not visible at the restrictive temperature (34.5°C), but actin patches remained. Scale bars: 1 µm. FRAP curves of Nup49–GFP-expressing thermosensitive tropomyosin (Δ*tpm2 tpm1-1*) mutant cells incubated at room temperature (RT) and 34.5°C. The curves are the mean±s.e.m.; Δ*tpm2 tpm1-1* (room temperature) *n*=39; Δ*tpm2 tpm1-1* (34.5°C) *n*=52. (D) FRAP analyses of Nup49–GFP in WT (*n*=37) and Δ*csm4* cells *n*=20. All nuclei were computationally aligned before the analyses to avoid biases owing to moving nuclei during recovery.

chromatin-remodeling complex INO80. As expected, the mobility of a centromeric locus was increased when Ino80 was targeted into its vicinity through the use of the LexA–Ino80 fusion ($C=4.76\times10^{-3}\pm2.84\times10^{-4}$ µm^2/s$^{0.5}$ versus $6.3\times10^{-3}\pm3.94\times10^{-4}$ for LexA and LexA–Ino80 transformed strains respectively; Fig. 5A, left). Following addition of latrunculin, the locus dynamics induced by LexA–Ino80 decreased and became similar to a control in which LexA alone had been targeted ($C=4.4\times10^{-3}\pm1.19\times10^{-4}$ µm^2/s$^{0.5}$ for LexA–Ino80 versus $C=4.3\times10^{-3}\pm1.21\times10^{-4}$ µm^2/s$^{0.5}$ for LexA alone; Fig. 5A, middle and right). Altogether, these results indicate that actin is essential for the Ino80-dependent increase in chromatin mobility.

Actin is required for efficient DNA repair through homologous recombination

Because actin is important for the regulation of chromosome dynamics by the chromatin-remodeling complex INO80, we hypothesized that DNA repair might be impaired in this context

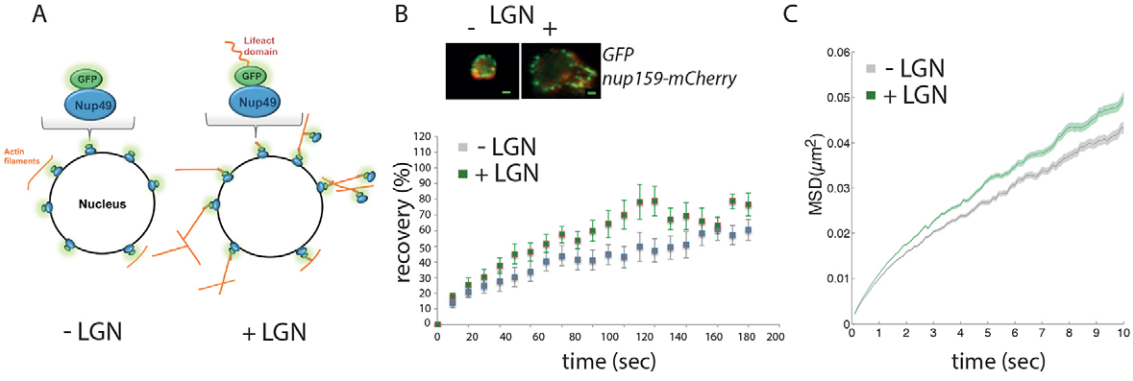

Fig. 3. Direct fusion of NPC to LifeAct increases nuclear pore mobility and subtelomere motion. (A) Schematic model of cells expressing LifeAct–GFP–Nup49 (+LGN) or not (–LGN). The actin cables surrounding the nucleus (–LGN) or linked to the nuclear pores through the LifeAct–Nup49–GFP fusion (+LGN) are shown. (B) Top, example of structured illuminated microscopy (SIM) image of a nucleus in cells expressing (or not) LGN and a Nup159–mCherry fusion (red). GFP, green. Scale bars: 1 µm. In the presence of LGN, deformation of the nucleus is visible. Bottom, FRAP analyses of Nup49–GFP in the presence or the absence of LGN. All nuclei were computationally aligned before the analyses to avoid biases owing to moving nuclei during recovery. The curves represent the mean±s.e.m.; –LGN, *n*=13; +LGN, *n*=10. (C) MSD of subtelomere Tel15R in the presence or the absence of LGN expression. MSD values after tracking spots in 2D time-lapse video (10 Hz) in 500–1000 cells. Nuclei displacements were corrected, and only one-third of the curve was taken into consideration to fit α and C (subdiffusion coefficient). Shaded area surrounding lines ±s.e.m..

Journal of Cell Science (2016) 129, 681-692 doi:10.1242/jcs.175745

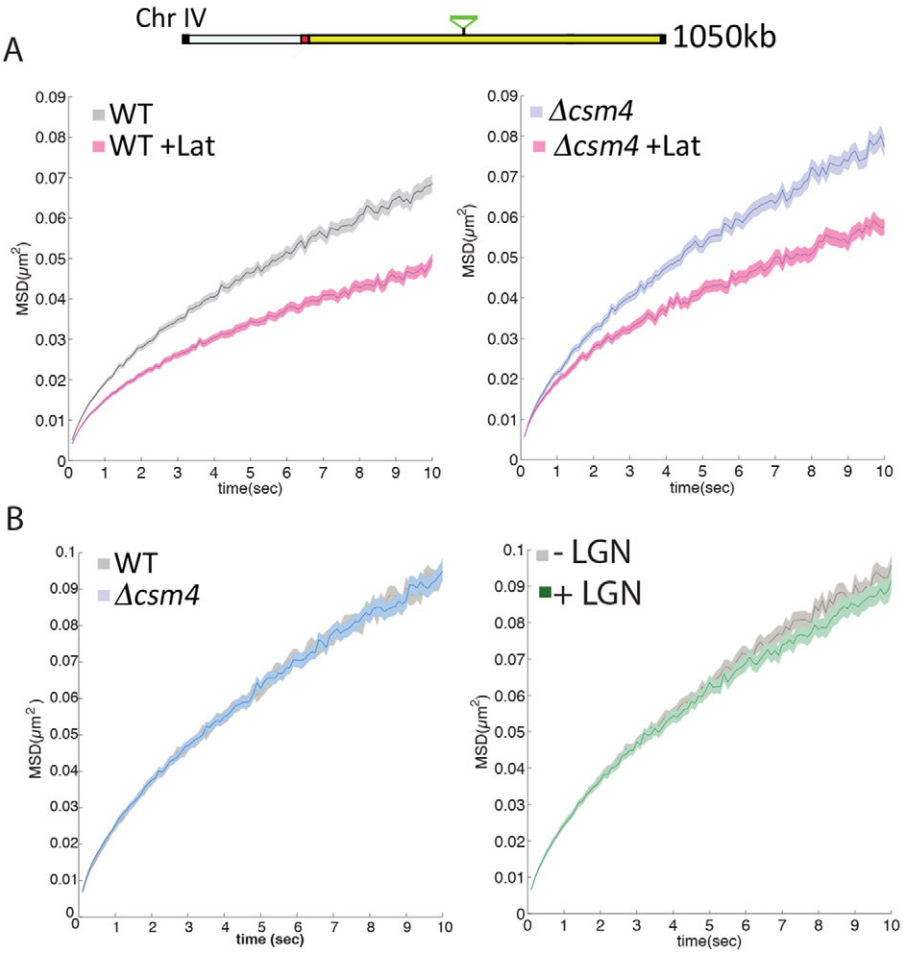

Fig. 4. The motion of an interstitial locus distant from the nuclear envelope is affected in the absence of polymerized actin but not in the absence of Csm4 or the presence of LGN. MSD values were calculated as described in Fig. 1. For annotation of schematic chromosome, also see Fig. 1. Yellow, right arm of chromosome IV. (A) MSD for a locus in the middle of the right arm of chromosome (Chr) IV in WT cells, in the absence (grey) or the presence of latrunculin A (Lat, pink), or in Δ*csm4* mutant cells in the absence (blue) or presence of latrunculin A (pink). (B) MSD values for the same locus in WT (grey) and Δ*csm4* cells (blue), or WT LGN-expressing cells (green). Shaded area surrounding lines ±s.e.m.

(Bennett et al., 2013). We therefore tested the efficiency of the homologous recombination repair pathway in the absence of filamentous actin. To do so, we turned to an ectopic recombination assay where a HO-endonuclease-induced DSB is generated within a recipient cassette carrying sequences identical to a donor cassette positioned elsewhere in the genome (Agmon et al., 2013; Aylon et al., 2004). DSB and homologous recombination repair kinetics were quantified through semi-quantitative PCR amplification (Fig. 5B, Materials and Methods; Agmon et al., 2013). Repair through homologous recombination between the donor and recipient cassettes is more efficient when both loci are positioned within subtelomeres of chromosome arms of similar sizes rather than of different sizes (Agmon et al., 2013). Using a strain in which both donor and recipient cassettes were positioned within the subtelomeres of short chromosome arms (Tel9R and an artificially truncated Tel13R-f; strain NA61-B8; Agmon et al., 2013), we performed a time-course experiment to measure repair through homologous recombination after HO-endonuclease induction in the absence and presence of latrunculin A (Materials and Methods). In a genetic WT background, the HO-endonuclease-induced DSBs at the recipient cassette were efficiently repaired using the donor cassette through homologous recombination (Fig. 5B, left). Interestingly, in the presence of latrunculin, cells conserved the ability to repair HO-endonuclease-induced DSBs through homologous recombination but with a lower efficiency (Fig. 5B, right). These results suggest that, although Tel9R and Tel13R-f share overlapping nuclear territories (Agmon et al., 2013), the proximity of homologous sequences is not sufficient for homologous repair to take place efficiently in the presence of latrunculin. The drop in the efficiency of homologous recombination in the presence of latrunculin A remains to be further characterized and could result from several mechanisms that are not mutually exclusive – the established role for actin in the INO80 complex (Agmon et al., 2013; Bennett et al., 2013; Horigome et al., 2014; Kapoor et al., 2013) – or a possible role in facilitating homology search through chromosome jiggling.

DISCUSSION

Although it has been established that chromatin is subject to Brownian as well as active motion, how the latter active processes are generated remains unclear. We show that during yeast interphase, both cytoplasmic and nuclear actin is required for dynamic motion of chromosomal loci. First, we provide an integrated and quantitative set of evidence that the nuclear envelope can transduce mechanical forces from the actin cytoskeleton to chromosome ends, promoting active dynamics. Second, we show that nuclear actin is required for the motion of loci that are positioned away from the nuclear membrane. Nuclear actin is involved in chromatin mobility and can act in association with the chromatin-remodeling complex INO80. Finally, we identify a role for actin in the homologous repair of DSBs.

Interphase subdiffusive chromatin dynamics requires actin

During the G1 stage of the cell cycle, subtelomeres localize principally at the nuclear periphery, centromeres are tethered to the SPB through nuclear microtubules and internal loci are

Journal of Cell Science (2016) 129, 681-692 doi:10.1242/jcs.175745

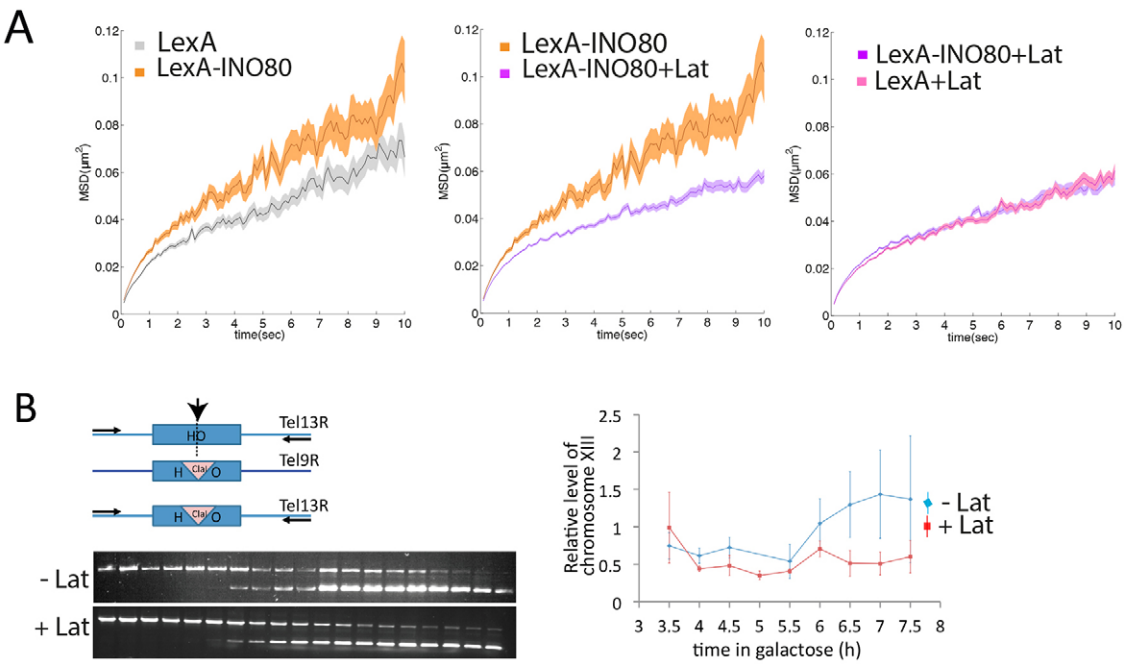

Fig. 5. An increase of Ino80-dependent chromatin mobility and DSB repair through homologous recombination depends on actin. MSD values were calculated as described in Fig. 1. (A) Left, MSDs for LexA-lacO repeats targeted at a position close to centromere of chromosome IV when LexA was expressed alone (grey) or with Ino80 (LexA–Ino80, orange), where LexA stand for LexA operators; middle, MSD values for the same position targeted by LexA–Ino80 in the absence (orange) or the presence of latrunculin A (violet, +Lat); right, MSD values for the same position targeted by LexA alone (pink) or LexA–Ino80 (violet) in the presence of latrunculin A (+Lat). (B) Kinetics of DSB repair are reduced in the absence of polymerized actin. Repair kinetics were analyzed by using quantitative PCR analysis of DNA obtained at different time intervals after transfer to galactose-containing medium in the presence or absence of latrunculin A (Lat). Left top, schematic of donor and recipient cassettes located, respectively, on a subtelomere of short chromosome IXR and truncated chromosome XIIIR, as previously described (Agmon et al., 2013). Left bottom, representative PCR results of the kinetics of the appearance of the gene conversion product. PCR products of chromosome XIII were digested with *Cla*I. Right, ratio of chromosome XIII amplification relative to that of a control locus (YPL200w), normalized to 1 at t0 (time of transfer to galactose), with or without latrunculin A (Lat). Curve is shown starting at 3 h. Data are averages of three independent experiments, and error bars show s.d.

preferentially found in the nuclear interior (Bystricky et al., 2005; Jin et al., 1998; Schober et al., 2008; Therizols et al., 2010; Verdaasdonk et al., 2013; Wong et al., 2012). We show that during G1, the motion of subtelomeric, peri-centromeric and interstitial loci is subdiffusive (exponent $\alpha \approx 0.5$). This is in agreement with previous studies, which have shown that locus motion does not obey free diffusion but is instead constrained with a subdiffusive behavior that is ubiquitously observed in bacteria, yeast and mammals (Heun et al., 2001; Marshall et al., 1997; Weber et al., 2012). The observed subdiffusive exponent is consistent with the Rouse model of polymer dynamics that assumes spring-like interactions between consecutive monomers, or alternatively with a viscoelastic response of the nuclear medium (Bronstein et al., 2009; Cabal et al., 2006; Hajjoul et al., 2013; Lucas et al., 2014; Weber et al., 2012). Although the anomalous exponent does not depend on the locus, the prefactor C shows variations relative to the genomic position, as exemplified by the reduced mobility of subtelomeres (Bystricky et al., 2005; Hajjoul et al., 2013; Heun et al., 2001). When actin filaments were depleted following addition of latrunculin A, the subdiffusive prefactor C was decreased, whereas the exponent $\alpha \approx 0.5$ was maintained, suggesting that actin filaments do not affect the constraint that prevents the locus from undergoing free diffusion. Consistent with previous work describing active ATP-dependent chromatin dynamics in yeast, our work establishes actin as a major driver of chromosome motion (Heun et al., 2001; Marshall et al., 1997; Steinberg et al., 2012; Weber et al., 2012). We failed to find directional movements, at least at the timescale we monitored (~100 ms; data not shown). Of note, in mammalian U2OS cells, small-sized actin filaments can be visualized, excluded from chromatin-rich regions, which lack any persistent directed motion (Belin et al., 2013). Our observations are nevertheless coherent with actin involvement in chromatin-based long-range motion that has been described in former studies in other eukaryotes (Chuang et al., 2006; Dundr et al., 2007).

The 32 yeast subtelomeres typically cluster into 3–6 transient foci of 2–3 subtelomeres, suggesting that a subset of chromosome ends are not colocalizing at any given time (Hoze et al., 2013; Schober et al., 2008; Therizols et al., 2010). The decrease of the volume of subtelomere territories in the absence of functional actin is associated with significant reductions in subtelomere dynamics and with an approximately 15% increase in subtelomere contacts, as detected by using 3C analysis. Hence, in the absence of actin-dependent motion, natural transient contacts are stabilized. This suggests a role for actin motion in the maintenance of subtelomere individualization through reducing subtelomere lifespan within foci. Interestingly, a potential role for the dynamic actin-mediated chromosome movements observed during yeast meiosis prophase has been found to solve unwanted entanglements and thus facilitate homolog pairing (Koszul et al., 2008; Koszul and Kleckner, 2009). Our observations suggest that such an influence of actin in maintaining individualization of chromosomes might extend to the vegetative cell cycle as well.

Interplay between actin filaments, the nuclear envelope and chromosomes

The nuclear envelope is a complex structure comprising a lipid bilayer and protein complexes that separates the nucleoplasm from the cytoplasm. During budding yeast meiosis, a protein complex

Journal of Cell Science (2016) 129, 681-692 doi:10.1242/jcs.175745

spanning through the nuclear envelope transmits mechanical forces from the actin cytoskeleton to chromosome ends, resulting in dynamic motion of the entire chromosome. The motion observed during interphase differs dramatically in its amplitude from the one that has been characterized during meiosis. During meiotic prophase, actin-dependent localization and dynamics of telomeres is impaired in the absence of either Csm4 (a putative KASH-like protein), the N-terminal region of Mps3 (SUN-like protein, $\Delta_{75\text{-}150}$mps3) or Ndj1, a meiotic telomere binding protein (Conrad et al., 2008; Koszul et al., 2008; Trelles-Sticken et al., 2005; Scherthan et al., 2007). In G1, Csm4 also influenced subtelomere organization and dynamics – in the mutant, the motion of delocalized subtelomere was increased, rather than reduced as it is in meiosis. The role of Csm4 in transducing a mechanical force from the cytoskeleton to chromosomes during meiosis prophase thus remains specific to that stage. The NPC was recently reported as being an additional intermediate between cytoskeleton forces and chromatin in the nuclear envelope. Cytoplasmic molecular motors in both *S. cerevisiae* and *Ustilago Maydis* have been shown to prevent NPC clustering and to affect chromosome distribution (Steinberg et al., 2012). We did not observe such clustering in the absence of actin filaments in our strain backgrounds, but we observed slower nuclear pore mobility under actin-depolymerizing conditions. The deletions of *DYN2* or *PAC11* reduce NPC mobility (Steinberg et al., 2012), and Dyn2 and Pac11, which interact with Act1 and proteins of the NPCs (Stelter et al., 2007), might therefore be good candidates for establishing a bridge between actin cables and NPCs. In contrast, Pom152 and Nup170 have no effect on NPC mobility, although interactions between Nup170 and subtelomeres have recently been documented (Van de Vosse et al., 2013). Overall, these results are consistent with a pivotal role of the NPC in the regulation of subtelomere dynamics during interphase.

To test the role of the NPC as an intermediate between the actin cytoskeleton and chromosomes, two experiments were performed. First, using FRAP, we determined that the mobility of the NPC was decreased in the absence of actin filaments (both after latrunculin A addition or tropomyosin inactivation), establishing a link between actin and NPC dynamics. Second, we showed that increasing the connections of actin to the NPC increases subtelomere dynamics, pointing at a connection between NPC and chromatin. Subtelomere motion in WT cells therefore results, at least in part, from the dynamic interplay between the actin cytoskeleton, the NPC and chromosomes. Interestingly, in mammals, distinct cytoskeleton motors – i.e. the microtubules – have been recently shown to transduce a mechanical force through the LINC complex to increase the chromosome mobility of nearby damaged telomeres (Lottersberger et al., 2015).

A role for nuclear actin in chromatin mobility

Studying the influence of actin on nuclear processes is an intrinsically difficult task because every manipulation of cytoplasmic actin-cable depolymerization affects the equilibrium between G-actin and F-actin in the cell. This includes treatment with latrunculin A (Domazetovska et al., 2007; Schoenenberger et al., 2005). Therefore, techniques that tether cytoplasmic actin to a nucleoporin (Fig. 3), for example, appears to be a promising approach to distinguish between cytoplasmic and nuclear actin. Yet, the observation that latrunculin A affects the mobility of loci that are positioned away from the nuclear envelope (i.e. delocalized subtelomeres in the Δ*csm4* mutant or interstitial chromosomal loci) suggests that the forces generated at the cytoplasm level are not the only players in chromatin mobility and prompted us to test for a role of actin in the nucleus. We found that a fusion protein comprising actin and the LexA-binding domain under the control of a conditional promoter has a dominant-negative effect on cytoplasmic actin (data not shown). We therefore exploited the fusion between chromatin remodeling protein Ino80 and the LexA-binding protein (Neumann et al., 2012) to target Ino80 to LexA-binding sites. The increase in local chromatin mobility required the ATPase activity of Ino80 (Neumann et al., 2012) but was suppressed by the addition of latrunculin, showing that actin is also required for INO80 complex function. How actin acts in the remodeling complex to increase dynamics remains an open question, but it is known that, *in vitro*, an *act1-2* mutant has a decreased affinity for chromatin and that latrunculin A might affect actin ATPase activity by binding to actin barbed ends (Morton et al., 2000). Because Ino80 is targeted to chromatin by LexA, we propose that defective chromatin motion due to latrunculin A binding to actin might not happen through a defective binding of the INO80 complex to chromatin but rather through the inability to assemble a functional INO80 complex.

Functional consequences

The addition of latrunculin A during meiosis prophase impairs the proper progression of the carefully regulated meiotic program. We found that actin-dependent chromosome movements affect homologous recombination repair efficiency. This repair mechanism requires the recruitment of INO80, SWR-C, NuA4, SWI/SNF and RSC to the DSBs during S phase (Bennett et al., 2013). Interestingly, the INO80, SWR-C and NuA4 complexes contain actin in both yeast and mammals (for review, see Kapoor and Shen, 2014). Of these three remodeling complexes, only the ATPase subunit of INO80 has been found to induce a local increase of mobility (Neumann et al., 2012). It is unknown at this stage if actin is affected to a similar extent in all remodeling complexes by the addition of latrunculin. It will be challenging to distinguish whether efficient repair requires local mobility, the presence of functional chromatin-remodeling complexes or both. Drug inhibition of actin under DSB-inducing conditions leads to chromosome fragmentation, indicating another role for actin in DNA repair (Shimada et al., 2013). Interestingly, a recent study in U2OS cells shows that nuclear actin filaments are generated upon DSB induction and, in turn, these filaments are required for efficient repair (Belin et al., 2015). A role of actin in DSB repair, perhaps through its function in chromatin dynamics, appears to be an evolutionarily conserved feature.

Overall, the present study shows that chromatin mobility during interphase requires actin. Our results open interesting perspectives regarding the interplay between cytoskeleton and chromosome organization, and the role of nuclear actin in chromatin-remodeling complexes. It is becoming increasingly clear that mechano-sensing mechanisms are able to transduce mechanical signals within and outside of the cells. For instance, signaling from the extracellular matrix to the nucleus has been described in mammals, and long nuclear filamentous structures that are sensitive to latrunculin A are associated with the NPCs of *Drosophila* oocytes, indicating intriguing interconnections that are likely to contribute to the complexity of cellular regulation (Kiseleva et al., 2004; Grinthal et al., 2010; Kumar et al., 2014).

MATERIALS AND METHODS

Yeast strains and plasmids

All strains are derivatives of BY4741 and listed in Table S2. Strains tagged for subtelomeres have been described previously by Therizols et al. (2010). These strains were additionally marked for the SPB with *SPC29-mCherry* through PCR transformation and for the nuclear envelope with a plasmid

Journal of Cell Science (2016) 129, 681-692 doi:10.1242/jcs.175745

containing *NUP49-GFP-ADE2*. *Δtpm2*, *tpm1-1* mutant was obtained from I. Sagot Université de Bordeaux, Institut de Biochimie et Génétique Cellulaires, Bordeaux, France. Mutants (*Δcsm4*, *Δpom152*, *Δnup170* and *Δarp8*) were from the Euroscarf collection.

LifeAct–GFP and LifeAct–GFP–Nup49 fusions were constructed according to the Gilson method. Overlapping PCRs from LifeAct, GFP or Nup49, and replicative plasmids containing ADE2 or KANMX were used to transform yeast. Plasmids were purified from yeast transformants, amplified in *Escherichia coli* and verified by sequencing.

Centrifugal elutriation

For cell-cycle synchronization in G1 phase, cells that had been grown in synthetic complete (SC) medium to exponential phase were harvested and resuspended in 30 ml of PBS (1×10^{10}–1×10^{11} cells) and loaded into the chamber (Sanderson elutriation chamber; Beckman Coulter) at a flow rate of 20 ml/min and a rotor speed of 602 ***g***, at 23°C. The elutriation chamber was filled by increasing the flow rate by 2 ml/min, followed by 1 h of cell equilibration. 50 ml were collected per fraction. The cell-cycle stage was determined on a subfraction by using fluorescence-activated cell sorting (FACS) using MACSQuant (Miltenyi) and FlowJo software. For imaging, cells were incubated for 10 min in SC medium and budding was observed after 30 min.

Growth conditions, live imaging and image analysis

For live imaging, overnight cultures in appropriate culture medium (SC medium) were diluted 1:50 and grown for two generations. Cells were patched onto SC medium containing 2% agar. Cover slides were sealed with 1/3 vaseline, 1/3 lanoline and 1/3 paraffin (VaLaP). To depolymerize actin, latrunculin A was dissolved in DMSO at 30 µM and added to cells for 30 min. Exceptions were for cells used to generate gene maps, which were treated with latrunculin B (latrunculin B, Invitrogen Molecular Probes) dissolved in DMSO at 100 µM and incubated for 10 min. Control experiments were in the presence of the solvent. For LexA–Ino80 induction experiments, cells that had been grown in exponential phase in SC-Leu drop-out medium containing doxycycline (Dox) at 10 µg/ml, were washed once in SC-Leu drop-out medium without Dox and left to grow for 2 h. 3D images were captured as described previously (Therizols et al., 2010).

Stacks with a slice spacing of 300 nm were taken at an acquisition time of 200 ms for each wavelength excitation. Powers of diode pumped solid-state laser (DPSSL) were 75% for 488-nm excitation and 100% for 560 nm.

Images were analyzed with the nucloc software (Berger et al., 2008) modified to use the SPB as a nuclear landmark. All 3D distances were computed after correction for chromatic aberrations. Locus probability maps were generated using kernel density estimation, and contours corresponded to percentiles of cells (Therizols et al., 2010). When comparing two locus probability maps, a *P*-value was attributed for the null hypothesis that the probability densities were identical.

For 2D locus tracking, cells were imaged for 100 ms at 100% for 488-nm excitation for the TetO/TetR–GFP insertions and 100 ms at 100% for 560-nm excitation for Spc29–mCherry with a Nikon fluorescence microscope (Camera Andor Neo sCMOS, software Andor IQ2 2.7.1, LED Lumencor Spectra X). At least 200 nuclei were tracked for 30 s.

2D locus trajectories were computed using an in-house ImageJ tracking plugin. The program located the locus and the center of the nucleus and corrected for the motion of the nucleus. The MSD values were computed using non-overlapping time intervals and fitted to power laws $MSD=C\times4\Delta t^{\alpha}$ using Matlab. To minimize statistical uncertainty, the fit was performed on the first third of the total duration of the experiment. Here, Δt is time interval, α is an exponent characterizing the motion ($\alpha=1$ for normal diffusion, $\alpha<1$ for subdiffusion) and C is a constant coefficient that corresponds to the diffusion coefficient for $\alpha=1$. Because we consistently obtained $\alpha\approx0.5$, the power law with the exponent was fixed to 0.5 ($MSD=C\times4\Delta t^{0.5}$) to obtain C values with the same units.

Fluorescence recovery after photobleaching

FRAP experiments were performed with an inverted confocal microscope UltraView ERS (26-01-08e). Samples were excited with a 488-nm laser at 100% for 800 ms. After recording five pre-bleach images, nuclei were bleached by the bleaching device at 488 nm at 100% for 50 ms. Post-bleaching images were taken every 10 s for 5 min. Nuclear drift was corrected by using the StackReg function in ImageJ, and fluorescence recovery was quantified using a Matlab program that computed: $I_{norm}(t)=(I_{frap}(t)-I_{back}(t))/I_{frap\_pre}$, where $I_{frap}(t)$ is the intensity of the FRAP region at time t, I_{back} is the intensity of the background region, I_{norm} is the normalized intensity, I_{frap_pre} is the pre-bleach intensity.

DNA repair assay

This assay was performed as described previously, using strain NA61-B8 (Agmon et al., 2013). This strain contains a 1.2-kb recipient cassette (KanMX::HO-cs) and a homologous donor cassette (KanMX::ClaI). The strain also contains a GAL-inducible HO endonuclease. Cells were grown in YPLac medium at 30°C to exponential phase. Cells were then centrifuged and incubated in 30 µM latrunculin A for 30 min or the equivalent volume of DMSO when 2% galactose was added. Subsequently, cells were diluted in YPGal medium, and samples were taken every 30 min for semi-quantitative PCR analysis with primers against Tel13R (Agmon et al., 2013). Control PCR analyses were performed using primers for the gene *CSM4*. After electrophoresis, bands were quantified using ImageJ.

Generation of 3C libraries and generation of contact matrices

3C libraries were prepared as described previously by Marie-Nelly et al. (2014). Cells that had been treated with 30 µM latrunculin A or DMSO were subjected to crosslinking with 3% formaldehyde for 30 min. 3C libraries were sheared after digestion with *Dpn*II, and fragments of 400–800 bp were sequenced using 100-bp pair-end sequencing on an Illumina HiSeq2000. Genome-wide 3C matrices were built with bins of 1 restriction fragment and normalized with Sequential Component Normalization after filtering of non-relevant events for 3D information and removing poor interacting bins. Specific subtelomere matrices were constructed by taking 100 bins, representing about 35 kb, for each subtelomeric region. Each interaction between two different subtelomeric regions is the average of interaction scores between the bins belonging to two subtelomeric regions resulting in a 32×32 matrix. For each pair of vectors i,j, the (i,i) and (j,j) elements were set to zero and the (i,j) and (j,i) elements were positioned so that both vectors had the same order in the interactions. The correlation matrix was calculated by taking the Pearson coefficient between each pair of vectors using the cor function of R with complete method. Subtelomeres were divided into three groups according to the size of the chromosome arm. The matrix representing interactions of the three different categories was obtained by calculating the average of elements of the correlation matrix between each group. To generate the plot of interactions along the subtelomeric region, genome-wide 3C matrices were built and normalized to represent the interactions between subtelomeres along this region, comprising the first 20 or the last 20 bins of each chromosome (representing about 35 kb). 3C matrices were built as described above, except that bins of five restriction fragments were used. For each bin inside a subtelomeric region, the interaction score was the average of the interactions with the bins from other subtelomeres. The final signal is the average of all subtelomeric regions. For the random set, an equal number of bins were chosen at random in the genome.

Acknowledgements

We are indebted to Tarn Duong for statistical analyses of gene maps, Florian Muller for help in FRAP analyses, Rudy Ruis for help in SIM acquisitions at Curie's Institute Nikon platform, Joachim Goedhart for the LifeAct-containing plasmid (Swammerdam Institute for Life Sciences, University of Amsterdam, Amsterdam, The Netherlands), Susan Gasser for LexA–Ino80 plasmids (Friedrich Miescher Institute for Biomedical Research, Basel, Switzerland), Catherine Dargemont for the NUP159–mCherry-containing strain (Laboratory of Pathology and Molecular Virology, Institut Universitaire d'Hématologie, Paris, France) and Isabelle Sagot for tropomyosin mutant strain (Institut de Biochimie et Génétique Cellulaires, Université de Bordeaux, Bordeaux, France). We thank Pierre Therizols and Isabelle Sagot for their critical reading, and Adeline Veillet for improving the manuscript.

Competing interests

The authors declare no competing or financial interests.

Author contributions

M.S., A.B. and M.B. performed the experiments, S.H. established the dynamics settings, A.C. analyzed the 3C data, C.Z. analyzed the dynamics data , R.K and E.F. conceived the experiments, analyzed the data and wrote the paper. A.B. and S.H. contributed equally to the research.

Funding

This research was supported by funding to R.K. from the European Research Council under the 7th Framework Program [grant numbers FP7/2007-2013 and ERC grant agreement number 260822]; and to E.F. by Agence Nationale de la Recherche [grant numbers ANR-13-BSV8-0013-01 and ANR-13-BSV3-0012-03]; Agence pour la Recherche contre le Cancer (ARC) [grant number FI20121205474]; and Labex Who am I [grant number EE-2013]. C.Z. acknowledges funding from the Institut Pasteur and Fondation pour la Recherche Médicale (FRM). M.M. was supported by a fellowship from ARC [grant number 20100600373]; M.S. by a fellowship from Université Pierre et Marie Curie (UPMC) and the Ligue Nationale Contre le Cancer (LNCC), and S.H. was supported by the FRM.

Supplementary information

Supplementary information available online at
http://jcs.biologists.org/lookup/suppl/doi:10.1242/jcs.175745/-/DC1

References

Agmon, N., Liefshitz, B., Zimmer, C., Fabre, E. and Kupiec, M. (2013). Effect of nuclear architecture on the efficiency of double-strand break repair. *Nat. Cell Biol.* **15**, 694-699.

Aylon, Y., Liefshitz, B. and Kupiec, M. (2004). The CDK regulates repair of double-strand breaks by homologous recombination during the cell cycle. *EMBO J.* **23**, 4868-4875.

Baarlink, C., Wang, H. and Grosse, R. (2013). Nuclear actin network assembly by formins regulates the SRF coactivator MAL. *Science* **340**, 864-867.

Belin, B. J., Cimini, B. A., Blackburn, E. H. and Mullins, R. D. (2013). Visualization of actin filaments and monomers in somatic cell nuclei. *Mol. Biol. Cell,* **24**, 982-994.

Belin, B. J., Lee, T. and Mullins, R. D. (2015). DNA damage induces nuclear actin filament assembly by formin-2 and Spire-1/2 that promotes efficient DNA repair. *eLife* **4**, 1-37.

Bennett, G., Papamichos-Chronakis, M. and Peterson, C. L. (2013). DNA repair choice defines a common pathway for recruitment of chromatin regulators. *Nat. Commun.* **4**, 2084.

Berger, A. B., Cabal, G. G., Fabre, E., Duong, T., Buc, H., Nehrbass, U., Olivo-Marin, J.-C., Gadal, O. and Zimmer, C. (2008). High-resolution statistical mapping reveals gene territories in live yeast. *Nat. Methods* **5**, 1031-1037.

Bronstein, I., Israel, Y., Kepten, E., Mai, S., Shav-Tal, Y., Barkai, E. and Garini, Y. (2009). Transient anomalous diffusion of telomeres in the nucleus of mammalian cells. *Phys. Rev. Lett.* **103**, 018102.

Bupp, J. M., Martin, A. E., Stensrud, E. S. and Jaspersen, S. L. (2007). Telomere anchoring at the nuclear periphery requires the budding yeast Sad1-UNC-84 domain protein Mps3. *J. Cell Biol.* **179**, 845-854.

Bystricky, K., Laroche, T., van Houwe, G., Blaszczyk, M. and Gasser, S. M. (2005). Chromosome looping in yeast: telomere pairing and coordinated movement reflect anchoring efficiency and territorial organization. *J. Cell Biol.* **168**, 375-387.

Cabal, G. G., Genovesio, A., Rodriguez-Navarro, S., Zimmer, C., Gadal, O., Lesne, A., Buc, H., Feuerbach-Fournier, F., Olivo-Marin, J.-C., Hurt, E. C. et al. (2006). SAGA interacting factors confine sub-diffusion of transcribed genes to the nuclear envelope. *Nature* **441**, 770-773.

Chuang, C.-H. and Belmont, A. S. (2007). Moving chromatin within the interphase nucleus-controlled transitions? *Semin. Cell Dev. Biol.* **18**, 698-706.

Chuang, C.-H., Carpenter, A. E., Fuchsova, B., Johnson, T., de Lanerolle, P. and Belmont, A. S. (2006). Long-range directional movement of an interphase chromosome site. *Curr. Biol.* **16**, 825-831.

Conrad, M. N., Lee, C.-Y., Chao, G., Shinohara, M., Kosaka, H., Shinohara, A., Conchello, J.-A. and Dresser, M. E. (2008). Rapid telomere movement in meiotic prophase is promoted by NDJ1, MPS3, and CSM4 and is modulated by recombination. *Cell* **133**, 1175-1187.

de Lanerolle, P. (2012). Nuclear actin and myosins at a glance. *J. Cell Sci.* **125**, 4945-4949.

de Lanerolle, P. and Serebryannyy, L. (2011). Nuclear actin and myosins: life without filaments. *Nat. Cell Biol.* **13**, 1282-1288.

Dion, V. and Gasser, S. M. (2013). Chromatin movement in the maintenance of genome stability. *Cell* **152**, 1355-1364.

Domazetovska, A., Ilkovski, B., Cooper, S. T., Ghoddusi, M., Hardeman, E. C., Minamide, L. S., Gunning, P. W., Bamburg, J. R. and North, K. N. (2007). Mechanisms underlying intranuclear rod formation. *Brain* **130**, 3275-3284.

Drees, B., Brown, C., Barrell, B. G. and Bretscher, A. (1995). Tropomyosin is essential in yeast, yet the TPM1 and TPM2 products perform distinct functions. *J. Cell Biol.* **128**, 383-392.

Duan, Z., Andronescu, M., Schutz, K., McIlwain, S., Kim, Y. J., Lee, C., Shendure, J., Fields, S., Blau, C. A. and Noble, W. S. (2010). A three-dimensional model of the yeast genome. *Nature* **465**, 363-367.

Dundr, M., Ospina, J. K., Sung, M.-H., John, S., Upender, M., Ried, T., Hager, G. L. and Matera, A. G. (2007). Actin-dependent intranuclear repositioning of an active gene locus in vivo. *J. Cell Biol.* **179**, 1095-1103.

Duong, T., Goud, B. and Schauer, K. (2012). Closed-form density-based framework for automatic detection of cellular morphology changes. *Proc. Natl. Acad. Sci. USA* **109**, 8382-8387.

Feuerbach, F., Galy, V., Trelles-Sticken, E., Fromont-Racine, M., Jacquier, A., Gilson, E., Olivo-Marin, J.-C., Scherthan, H. and Nehrbass, U. (2002). Nuclear architecture and spatial positioning help establish transcriptional states of telomeres in yeast. *Nat. Cell Biol.* **4**, 214-221.

Galy, V., Olivo-Marin, J.-C., Scherthan, H., Doye, V., Rascalou, N. and Nehrbass, U. (2000). Nuclear pore complexes in the organization of silent telomeric chromatin. *Nature* **403**, 108-112.

Grinthal, A., Adamovic, I., Weiner, B., Karplus, M. and Kleckner, N. (2010). PR65, the HEAT-repeat scaffold of phosphatase PP2A, is an elastic connector that links force and catalysis. *Proc. Natl. Acad. Sci. USA* **107**, 2467-2472.

Grosse, R. and Vartiainen, M. K. (2013). To be or not to be assembled: progressing into nuclear actin filaments. *Nat. Rev. Mol. Cell Biol.* **14**, 693-697.

Hajjoul, H., Mathon, J., Ranchon, H., Goiffon, I., Mozziconacci, J., Albert, B., Carrivain, P., Victor, J.-M., Gadal, O., Bystricky, K. et al. (2013). High-throughput chromatin motion tracking in living yeast reveals the flexibility of the fiber throughout the genome. *Genome Res.* **23**, 1829-1838.

Hayakawa, A., Babour, A., Sengmanivong, L. and Dargemont, C. (2012). Ubiquitylation of the nuclear pore complex controls nuclear migration during mitosis in S. cerevisiae. *J. Cell Biol.* **196**, 19-27.

Hediger, F., Neumann, F. R., Van Houwe, G., Dubrana, K. and Gasser, S. M. (2002). Live imaging of telomeres. yKu and sir proteins define redundant telomere-anchoring pathways in yeast. *Curr. Biol.* **12**, 2076-2089.

Heun, P., Laroche, T., Shimada, K., Furrer, P. and Gasser, S. M. (2001). Chromosome dynamics in the yeast interphase nucleus. *Science* **294**, 2181-2186.

Hiraga, S.-i., Botsios, S. and Donaldson, A. D. (2008). Histone H3 lysine 56 acetylation by Rtt109 is crucial for chromosome positioning. *J. Cell Biol.* **183**, 641-651.

Horigome, C., Oma, Y., Konishi, T., Schmid, R., Marcomini, I., Hauer, M. H., Dion, V., Harata, M. and Gasser, S. M. (2014). SWR1 and INO80 chromatin remodelers contribute to DNA double-strand break perinuclear anchorage site choice. *Mol. Cell* **55**, 626-639.

Horn, H. F., Kim, D. I., Wright, G. D., Wong, E. S. H., Stewart, C. L., Burke, B. and Roux, K. J. (2013). A mammalian KASH domain protein coupling meiotic chromosomes to the cytoskeleton. *J. Cell Biol.* **202**, 1023-1039.

Hoze, N., Ruault, M., Amoruso, C., Taddei, A. and Holcman, D. (2013). Spatial telomere organization and clustering in yeast Saccharomyces cerevisiae nucleus is generated by a random dynamics of aggregation-dissociation. *Mol. Biol. Cell* **24**, 1791-1800.

Jin, Q.-w., Trelles-Sticken, E., Scherthan, H. and Loidl, J. (1998). Yeast nuclei display prominent centromere clustering that is reduced in nondividing cells and in meiotic prophase. *J. Cell Biol.* **141**, 21-29.

Kapoor, P. and Shen, X. (2014). Mechanisms of nuclear actin in chromatin-remodeling complexes. *Trends Cell Biol.* **24**, 238-246.

Kapoor, P., Chen, M., Winkler, D. D., Luger, K. and Shen, X. (2013). Evidence for monomeric actin function in INO80 chromatin remodeling. *Nat. Struct. Mol. Biol.* **20**, 426-432.

Kiseleva, E., Drummond, S. P., Goldberg, M. W., Rutherford, S. A., Allen, T. D. and Wilson, K. L. (2004). Actin- and protein-4.1-containing filaments link nuclear pore complexes to subnuclear organelles in Xenopus oocyte nuclei. *J. Cell Sci.* **117**, 2481-2490.

Koszul, R. and Kleckner, N. (2009). Dynamic chromosome movements during meiosis: a way to eliminate unwanted connections? *Trends Cell Biol.* **19**, 716-724.

Koszul, R., Kim, K. P., Prentiss, M., Kleckner, N. and Kameoka, S. (2008). Meiotic chromosomes move by linkage to dynamic actin cables with transduction of force through the nuclear envelope. *Cell* **133**, 1188-1201.

Kumar, A., Mazzanti, M., Mistrik, M., Kosar, M., Beznoussenko, G. V., Mironov, A. A., Garrè, M., Parazzoli, D., Shivashankar, G. V., Scita, G. et al. (2014). ATR mediates a checkpoint at the nuclear envelope in response to mechanical stress. *Cell* **158**, 633-646.

Lottersberger, F., Karssemeijer, R. A., Dimitrova, N. and de Lange, T. (2015). 53BP1 and the LINC Complex Promote Microtubule- Dependent DSB Mobility and DNA Repair. *Cell* **163**, 880-893.

Lucas, J. S., Zhang, Y., Dudko, O. K. and Murre, C. (2014). 3D trajectories adopted by coding and regulatory DNA elements: first-passage times for genomic interactions. *Cell* **158**, 339-352.

Marbouty, M., Ermont, C., Dujon, B., Richard, G.-F. and Koszul, R. (2014). Purification of G 1 daughter cells from different Saccharomycetes species through an optimized centrifugal elutriation procedure. *Yeast* **31**, 159-166.

Marie-Nelly, H., Marbouty, M., Cournac, A., Liti, G., Fischer, G., Zimmer, C. and Koszul, R. (2014). Filling annotation gaps in yeast genomes using genome-wide contact maps. *Bioinformatics* **30**, 2105-2113.
Marshall, W. F., Straight, A., Marko, J. F., Swedlow, J., Dernburg, A., Belmont, A., Murray, A. W., Agard, D. A. and Sedat, J. W. (1997). Interphase chromosomes undergo constrained diffusional motion in living cells. *Curr. Biol.* **7**, 930-939.
Michaelis, C., Ciosk, R. and Nasmyth, K. (1997). Cohesins: chromosomal proteins that prevent premature separation of sister chromatids. *Cell* **91**, 35-45.
Mishra, M., Huang, J. and Balasubramanian, M. K. (2014). The yeast actin cytoskeleton. *FEMS Microbiol. Rev.* **38**, 213-227.
Morton, W. M., Ayscough, K. R. and McLaughlin, P. J. (2000). Latrunculin alters the actin-monomer subunit interface to prevent polymerization. *Nat. Cell Biol.* **2**, 376-378.
Neumann, F. R., Dion, V., Gehlen, L. R., Tsai-Pflugfelder, M., Schmid, R., Taddei, A. and Gasser, S. M. (2012). Targeted INO80 enhances subnuclear chromatin movement and ectopic homologous recombination. *Genes Dev.* **26**, 369-383.
Pruyne, D. W., Schott, D. H. and Bretscher, A. (1998). Tropomyosin-containing actin cables direct the Myo2p-dependent polarized delivery of secretory vesicles in budding yeast. *J. Cell Biol.* **143**, 1931-1945.
Riedl, J., Crevenna, A. H., Kessenbrock, K., Yu, J. H., Neukirchen, D., Bista, M., Bradke, F., Jenne, D., Holak, T. A., Werb, Z. et al. (2008). Lifeact: a versatile marker to visualize F-actin. *Nat. Methods* **5**, 605-607.
Rog, O. and Dernburg, A. F. (2013). Chromosome pairing and synapsis during Caenorhabditis elegans meiosis. *Curr. Opin. Cell Biol.* **25**, 349-356.
Scherthan, H., Wang, H., Adelfalk, C., White, E. J., Cowan, C., Cande, W. Z. and Kaback, D. B. (2007). Chromosome mobility during meiotic prophase in Saccharomyces cerevisiae. *Proc. Natl. Acad. Sci. USA* **104**, 16934-16939.
Schober, H., Kalck, V., Vega-Palas, M. A., Van Houwe, G., Sage, D., Unser, M., Gartenberg, M. R. and Gasser, S. M. (2008). Controlled exchange of chromosomal arms reveals principles driving telomere interactions in yeast. *Genome Res.* **18**, 261-271.
Schoenenberger, C.-A., Buchmeier, S., Boerries, M., Sütterlin, R., Aebi, U. and Jockusch, B. M. (2005). Conformation-specific antibodies reveal distinct actin structures in the nucleus and the cytoplasm. *J. Struct. Biol.* **152**, 157-168.
Sheehan, M. J. and Pawlowski, W. P. (2009). Live imaging of rapid chromosome movements in meiotic prophase I in maize. *Proc. Natl. Acad. Sci. USA* **106**, 20989-20994.
Shimada, K., Filipuzzi, I., Stahl, M., Helliwell, S. B., Studer, C., Hoepfner, D., Seeber, A., Loewith, R., Movva, N. R. and Gasser, S. M. (2013). TORC2 signaling pathway guarantees genome stability in the face of DNA strand breaks. *Mol. Cell* **51**, 829-839.
Soutoglou, E. and Misteli, T. (2007). Mobility and immobility of chromatin in transcription and genome stability. *Curr. Opin. Genet. Dev.* **17**, 435-442.
Steinberg, G., Schuster, M., Theisen, U., Kilaru, S., Forge, A. and Martin-Urdiroz, M. (2012). Motor-driven motility of fungal nuclear pores organizes chromosomes and fosters nucleocytoplasmic transport. *J. Cell Biol.* **198**, 343-355.
Stelter, P., Kunze, R., Flemming, D., Höpfner, D., Diepholz, M., Philippsen, P., Böttcher, B. and Hurt, E. (2007). Molecular basis for the functional interaction of dynein light chain with the nuclear-pore complex. *Nat. Cell Biol.* **9**, 788-796.
Stricker, J., Falzone, T. and Gardel, M. L. (2010). Mechanics of the F-actin cytoskeleton. *J. Biomech.* **43**, 9-14.
Taddei, A., Hediger, F., Neumann, F. R., Bauer, C. and Gasser, S. M. (2004). Separation of silencing from perinuclear anchoring functions in yeast Ku80, Sir4 and Esc1 proteins. *EMBO J.* **23**, 1301-1312.
Therizols, P., Fairhead, C., Cabal, G. G., Genovesio, A., Olivo-Marin, J.-C., Dujon, B. and Fabre, E. (2006). Telomere tethering at the nuclear periphery is essential for efficient DNA double strand break repair in subtelomeric region. *J. Cell Biol.* **172**, 189-199.
Therizols, P., Duong, T., Dujon, B., Zimmer, C. and Fabre, E. (2010). Chromosome arm length and nuclear constraints determine the dynamic relationship of yeast subtelomeres. *Proc. Natl. Acad. Sci. USA* **107**, 2025-2030.
Trelles-Sticken, E., Dresser, M. E. and Scherthan, H. (2000). Meiotic telomere protein Ndj1p is required for meiosis-specific telomere distribution, bouquet formation and efficient homologue pairing. *J. Cell Biol.* **151**, 95-106.
Trelles-Sticken, E., Adelfalk, C., Loidl, J. and Scherthan, H. (2005). Meiotic telomere clustering requires actin for its formation and cohesin for its resolution. *J. Cell Biol.* **170**, 213-223.
Van de Vosse, D. W., Wan, Y., Lapetina, D. L., Chen, W.-M., Chiang, J.-H., Aitchison, J. D. and Wozniak, R. W. (2013). A role for the nucleoporin Nup170p in chromatin structure and gene silencing. *Cell* **152**, 969-983.
Verdaasdonk, J. S., Vasquez, P. A., Barry, R. M., Barry, T., Goodwin, S., Forest, M. G. and Bloom, K. (2013). Centromere tethering confines chromosome domains. *Mol. Cell* **52**, 819-831.
Wanat, J. J., Kim, K. P., Koszul, R., Zanders, S., Weiner, B., Kleckner, N. and Alani, E. (2008). Csm4, in collaboration with Ndj1, mediates telomere-led chromosome dynamics and recombination during yeast meiosis. *PLoS Genet.* **4**, e1000188.
Weber, S. C., Spakowitz, A. J. and Theriot, J. A. (2010). Bacterial chromosomal loci move subdiffusively through a viscoelastic cytoplasm. *Phys. Rev. Lett.* **104**, 238102.
Weber, S. C., Spakowitz, A. J. and Theriot, J. A. (2012). Nonthermal ATP-dependent fluctuations contribute to the in vivo motion of chromosomal loci. *Proc. Natl. Acad. Sci. USA* **109**, 7338-7343.
Witkin, K. L., Friederichs, J. M., Cohen-Fix, O. and Jaspersen, S. L. (2010). Changes in the nuclear envelope environment affect spindle pole body duplication in Saccharomyces cerevisiae. *Genetics* **186**, 867-883.
Wong, H., Marie-Nelly, H., Herbert, S., Carrivain, P., Blanc, H., Koszul, R., Fabre, E. and Zimmer, C. (2012). A predictive computational model of the dynamic 3D interphase yeast nucleus. *Curr. Biol.* **22**, 1881-1890.
Zidovska, A., Weitz, D. A. and Mitchison, T. J. (2013). Micron-scale coherence in interphase chromatin dynamics. *Proc. Natl. Acad. Sci. USA* **110**, 15555-15560.
Zimmer, C. and Fabre, E. (2011). Principles of chromosomal organization: lessons from yeast. *J. Cell Biol.* **192**, 723-733.